Test Bench - Nano-Hexapod Struts

Dehaeze Thomas

April 8, 2024

Contents

The Nano-Hexapod struts (shown in Figure 1) each consists of:

- Two flexible joints that are fixed at the two ends of the strut
- One Amplified Piezoelectric Actuator (APA300ML)
- One encoder (Renishaw Vionic)

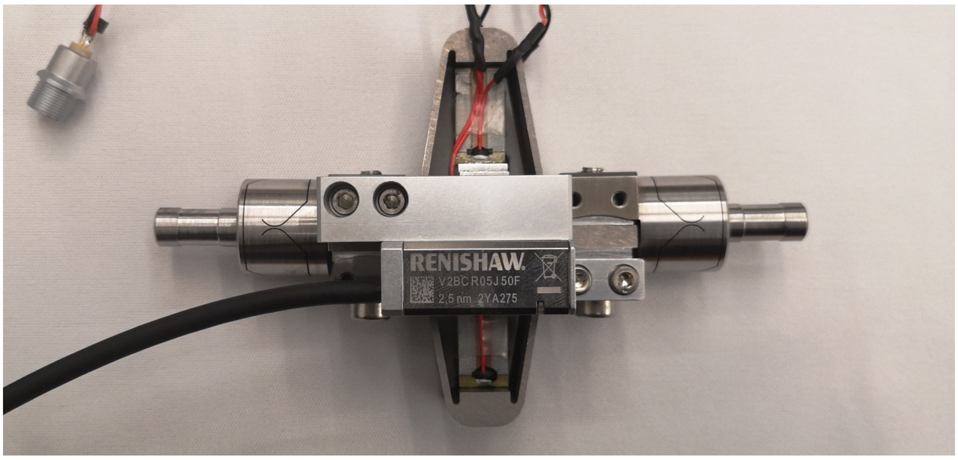

Figure 1: One strut including two flexible joints, an amplified piezoelectric actuator and an encoder

Now that all the strut elements have been individually characterized (see previous sections), the struts can be assembled. The mounting procedure of the struts is explained in Section 1. A mounting bench is used to ensure the coaxiality between the two ends of the struts. This way, no angular stroke is lost when mounted to the nano-hexapod.

Then the flexible modes of the struts are experimentally measured and compared with a finite element model (Section 2).

Dynamical measurements on the strut are performed with the same bench used to characterize the APA300ML dynamics in Section 3. It is found that the dynamics from DAC voltage to the displacement measured by the encoder is complex due to the flexible modes of the struts found in Section 2.

The models of the struts are then compared with the measured dynamics (Section 4). The model dynamics from the DAC voltage to the axial motion of the strut (measured by an interferometer) and to the force sensor voltage are matching well the experiment. However, this is not the case for the dynamics from DAC voltage to encoder displacement. It is found that the complex dynamics is due to a misalignment between the flexible joints and the APA.

Table 1: Report sections and corresponding Matlab files

Sections	**Matlab File**
Section 2	`test_struts_1_flexible_modes.m`
Section 3	`test_struts_2_dynamical_meas.m`
Section 4	`test_struts_3_simscape_model.m`

1 Mounting Procedure

A mounting bench has been develop to ensure:

- Good coaxial alignment between the interfaces (cylinders) of the flexible joints to minimize the angular stroke lost during their integration into the nano-hexapod
- Uniform length across all struts
- Precise alignment of the APA with the two flexible joints
- The assembly is reproducible and consistent from one strut to the other

1.1 Mounting Bench

A CAD view of the mounting bench is shown in Figure 1.1a. It consists of a “main frame” (Figure 1.2a) precisely machined to ensure both the correct strut length and strut coaxiality. The coaxiality is ensured by having good flatness (specified at $20\,\mu m$) between surfaces A and B, and between surfaces C and D. Such flatness has been checked using a Faro arm[1] (see Figure 1.2b) and was found to comply with the requirements. The strut length (defined by the distance between the rotation points of the two flexible joints) is ensured by using precisely machines dowel holes.

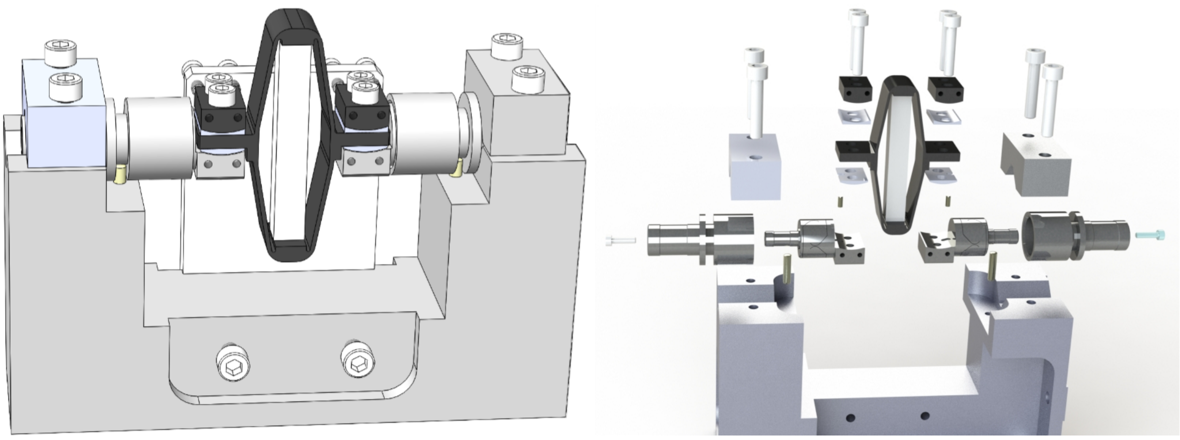

(a) CAD view of the mounting bench　　**(b)** Exploded view

Figure 1.1: Strut mounting bench

[1] Faro Arm Platinum 4ft, specified accuracy of $\pm 13 \mu m$

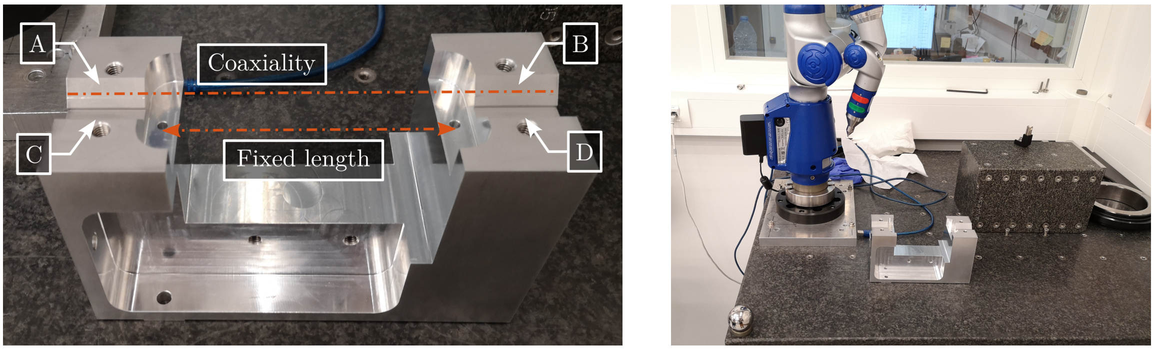

(a) Useful features of the main mounting element

(b) Dimensional check

Figure 1.2: Main element of the mounting bench for the struts that ensure good coaxility of the two flexible joints as well as the length of the struts.

The flexible joints are not directly fixed to the mounting bench but to to a cylindrical "sleeve" shown in Figures 1.3a and 1.3b. The goal of these "sleeves" is to avoid any mechanical stress that could damage the flexible joints during the mounting procedure. These "sleeves" have one dowel groove (that are fitted to the dowel holes shown in Figure 1.2a) that will determine the length of the mounted strut.

(a) Cylindral Interface (Top)

(b) Cylindrlcal Interface (Bottom)

(c) Mounted flexible joints

Figure 1.3: Preparation of the flexible joints by fixing them in their cylindrical "sleeve"

1.2 Mounting Procedure

The "sleeves" are mounted to the main element as shown in Figure 1.2a. The left sleeve has a thigh fit such that its orientation is fixed (it is roughly aligned horizontally) while the right sleeve has a loose fit such that it can rotate (it will get the same orientation as the fixed one when tightening the screws).

Then the cylindrical washers and the APA300ML are stacked on top of the flexible joints as shown in Figure 1.4b and screwed together using a torque screwdriver. A dowel pin is used to laterally align the APA300ML with the flexible joints (see the dowel slot on the flexible joints in Figure 1.3c). The two cylindrical washers are used to allow proper mounting even if the two APA interfaces are not parallel.

The encoder and ruler are then fixed to the strut and properly aligned as shown in Figure 1.4c.

Finally, the strut can be disassembled from the mounting bench (Figure 1.4d). Thanks to this mounting procedure, coaxiality and length between the two flexible joint's interfaces can be obtained within the wanted tolerances.

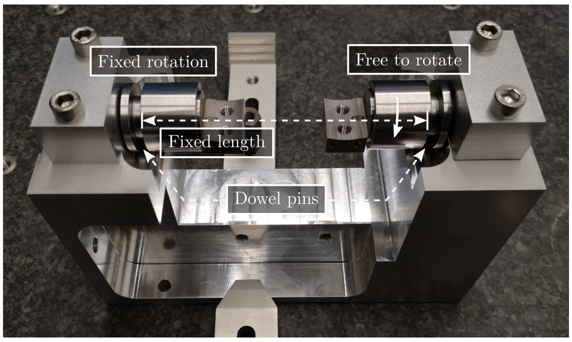

(a) Step 1

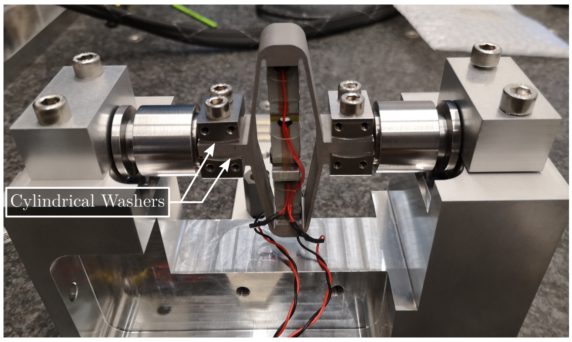

(b) Step 2

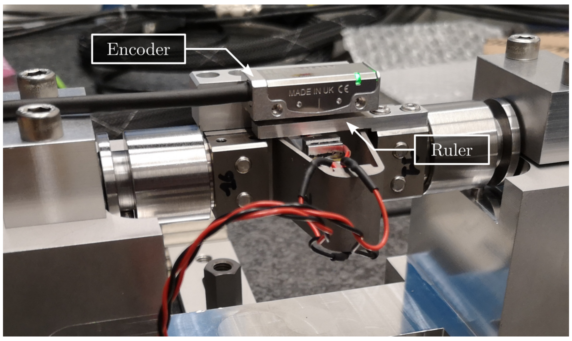

(c) Step 3

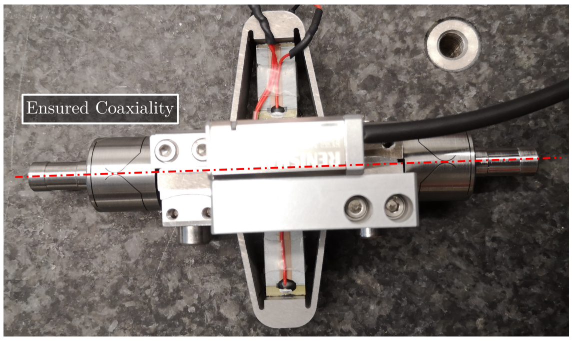

(d) Step 4

Figure 1.4: Steps for mounting the struts.

2 Measurement of flexible modes

2.1 Introduction

A Finite Element Model[1] of the struts is developed and is used to estimate the flexible modes. Inertia of the encoder (estimated at 15 g) is taken into account. The two cylindrical interfaces are fixed, and the first three flexible modes are computed. The modes shapes are displayed in Figure 2.1: an “X-bending” mode at 189Hz, a “Y-bending” mode at 285Hz and a “Z-torsion” mode at 400Hz.

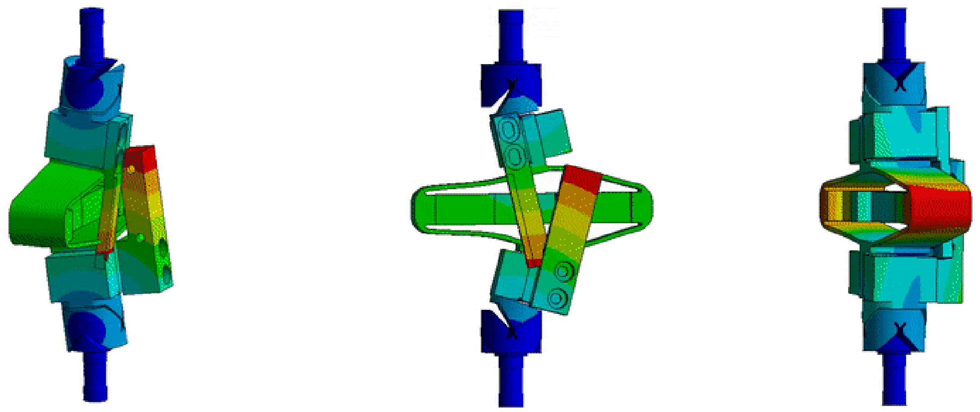

(a) X-bending mode (189Hz) **(b)** Y-bending mode (285Hz) **(c)** Z-torsion mode (400Hz)

Figure 2.1: Spurious resonances of the struts estimated from a Finite Element Model

2.2 Measurement Setup

In order to experimentally measure these mode shapes, a Laser vibrometer is used to measure the difference of motion between two beam path (red points in Figure 2.2). The strut is then excited with an instrumented hammer and the transfer function from the hammer to the measured rotation is computed.

The “X-bending” mode is measured as shown in Figure 2.2a. The “Y-bending” mode is measured as shown in Figure 2.2b. Finally, the “Z-torsion” is measured as shown in Figure 2.2c.

This is done with and without the encoder fixed to the strut.

[1]Using Ansys®. Flexible Joints and APA Shell material is stainless steel `1.4542`. Encoder and ruler support material is aluminium.

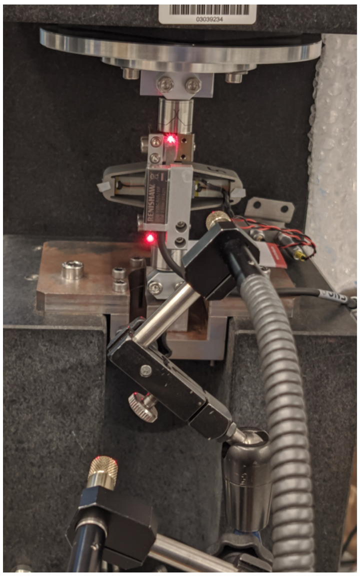

(a) X-bending mode

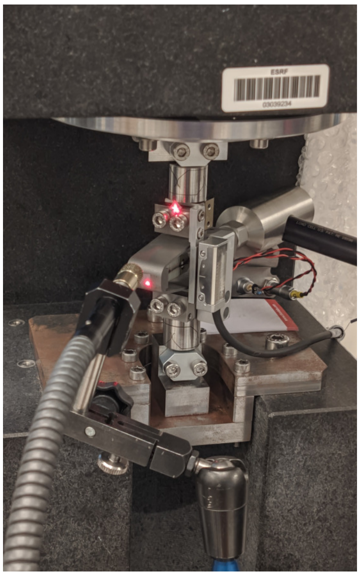

(b) Y-bending mode

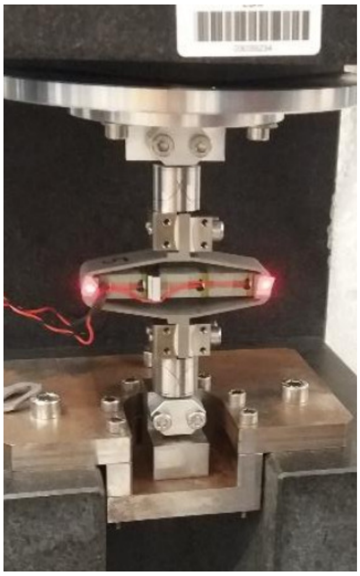

(c) Z-torsion mode

Figure 2.2: Measurement of strut flexible modes

2.3 Measured results

The obtained frequency response functions for the three configurations (X-bending, Y-bending and Z-torsion) are shown in Figure 2.3a when the encoder is not fixed to the strut and in Figure 2.3b when the encoder is fixed to the strut.

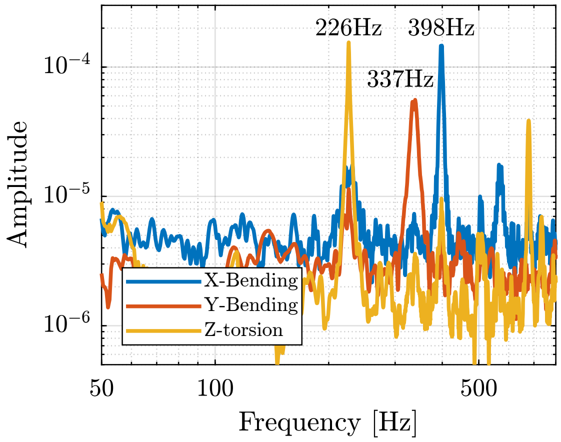

(a) without encoder

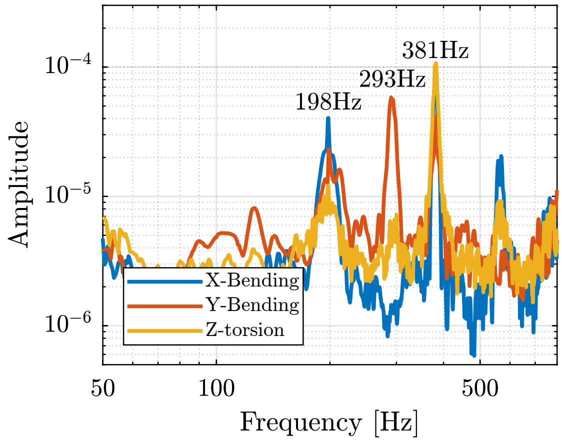

(b) with the encoder

Figure 2.3: Measured frequency response functions without the encoder 2.3 and with the encoder 2.3b

Conclusion

Table 2.1 summarizes the measured resonance frequencies as well as the computed ones using the Finite Element Model. It is shown that:

- the resonance frequencies of the 3 modes are only slightly decreased when the encoder is fixed to the strut
- the computed resonance frequencies from the FEM are very close to the measured one when the encoder is fixed to the strut

Table 2.1: Measured frequency of the flexible modes of the strut

Mode	**FEM with Encoder**	**Exp. with Encoder**	**Exp. without Encoder**
X-Bending	189Hz	198Hz	226Hz
Y-Bending	285Hz	293Hz	337Hz
Z-Torsion	400Hz	381Hz	398Hz

3 Dynamical measurements

In order to measure the dynamics of the strut, the same test bench used to measure the APA300ML dynamics is used.

The strut mounted on the bench is shown in Figure 3.1a A schematic of the bench and the associated signals are shown in Figure 3.1b. A fiber interferometer[1] is used to measure the motion of the granite (i.e. the axial motion of the strut).

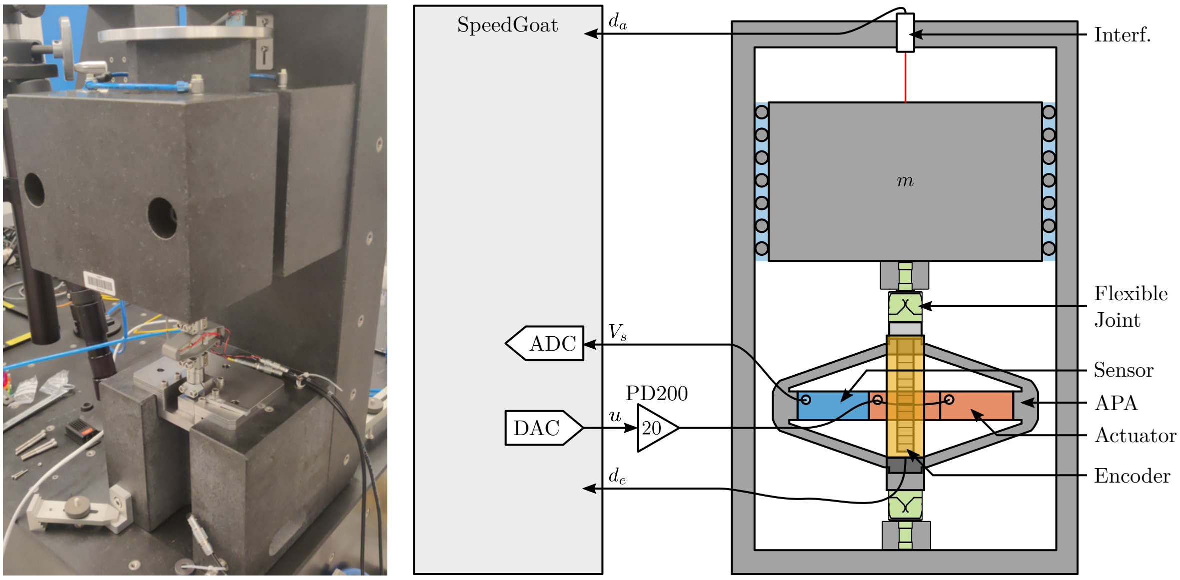

(a) Overview Picture

(b) Schematic

Figure 3.1: Experimental setup used to measured the dynamics of the struts.

First, the effect of the encoder on the measured dynamics is studied in Section 3.1. Then, the dynamics seen by the encoder and by the interferometers are compared in Section 3.2. Finally, all the measured struts are compared in terms of dynamics in Section 3.3.

3.1 Effect of the Encoder on the measured dynamics

System identification is performed in two cases:

- no encoder is fixed to the strut (Figure 3.2b)

[1] Two fiber intereferometers were used: an IDS3010 from Attocube and a quDIS from QuTools

- one encoder is fixed to the strut (Figure 3.2a)

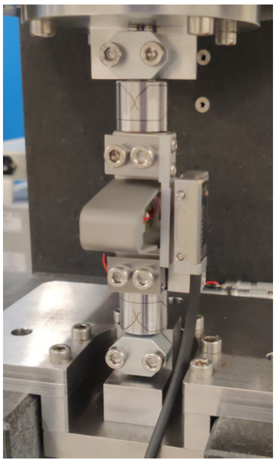

(a) Strut with encoder

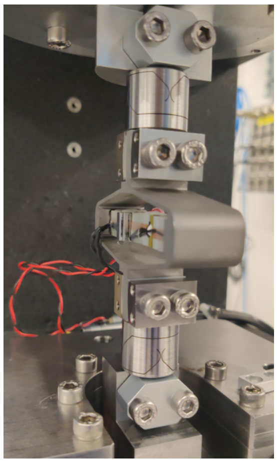

(b) Strut without encoder

Figure 3.2: Struts fixed to the test bench with clamped flexible joints. The coder can be fixed to the struts (a) or removed (b)

The obtained frequency response functions are compared in Figure 3.3. It is found that the encoder as very little effect on the transfer function from excitation voltage u to the axial motion of the strut d_a as measured by the interferometer (Figure 3.3a). This means that the axial motion of the strut is unaffected by the precense of the encoder. Similarly, it has very little effect on the transfer function from u to the sensor stack voltage V_s (Figure 3.3b). This means that the integral force feedback control strategy should be as effective whether or not the encoders are fixed to the struts.

3.2 Comparison of the encoder and interferometer

The dynamics as measured by the encoder and by the interferometers are compared in Figure 3.4.

The dynamics from the excitation voltage u to the measured displacement by the encoder d_e presents a behavior that is much more complex than the dynamics to the displacement as measured by the interferometer (comparison made in Figure 3.4). Three additional resonance frequencies can be observed at 197Hz, 290Hz and 376Hz. These resonance frequencies correspond to flexible modes of the strut that were studied in Section 2.

The good news is that these resonances are not seen on the interferometer and are therefore not impacting the axial motion of the strut (which is what is important for the hexapod positioning). However, these resonances are making the use of encoder fixed to the strut difficult.

3.3 Comparison of all the Struts

Then, the dynamics of all the mounted struts (only 5 at the time of the experiment) are all measured using the same test bench. The obtained dynamics from u to d_a are compared in Figure 3.5a while is

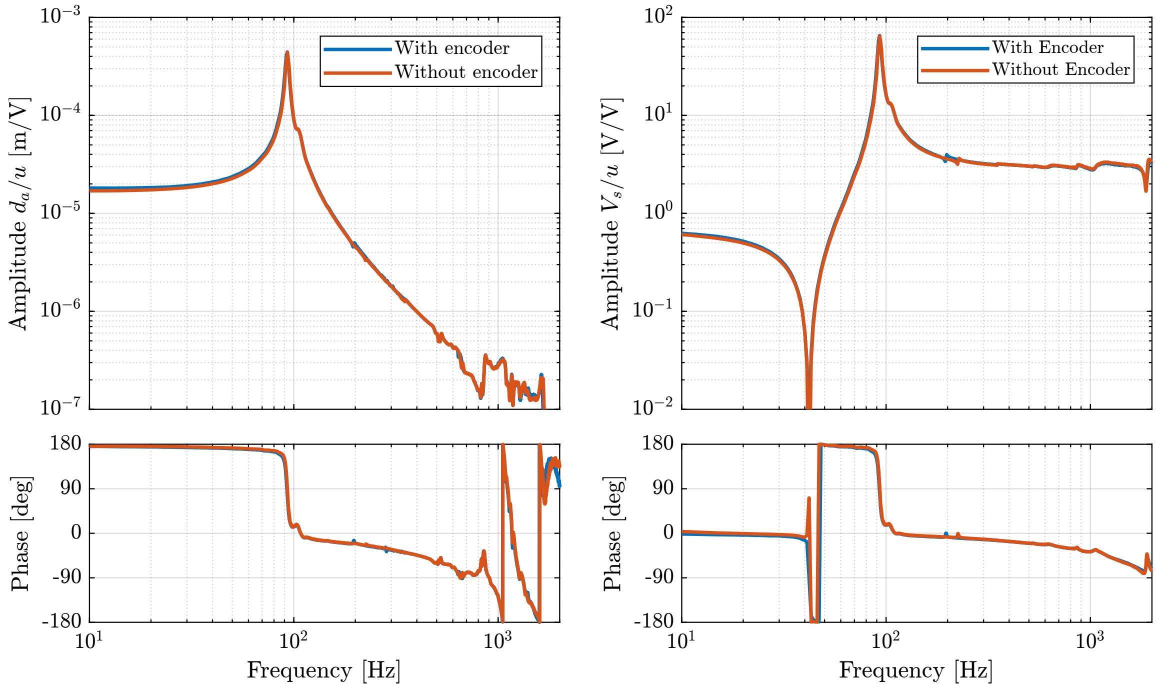

(a) u to d_a

(b) u to V_s

Figure 3.3: Effect of having the encoder fixed to the struts on the measured dynamics from u to d_a (a) and from u to V_s (b)

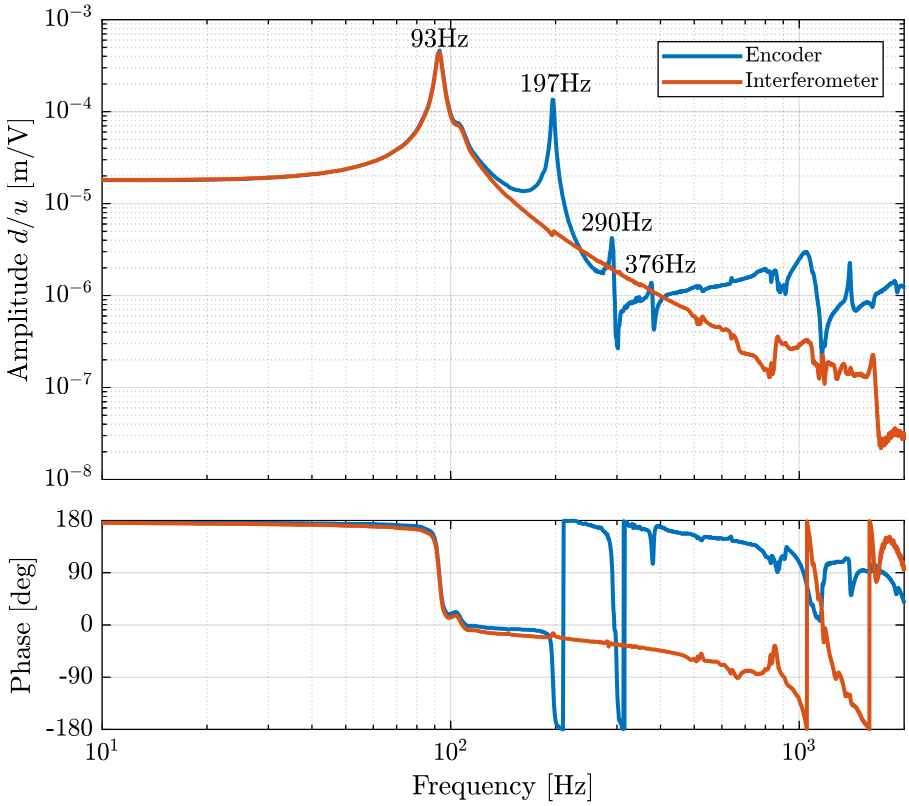

Figure 3.4: Comparison of the transfer functions from excitation voltage u to either the encoder d_e or the interferometer d_a

dynamics from u to V_s are compared in Figure 3.5b. Very good match can be observed between all the struts.

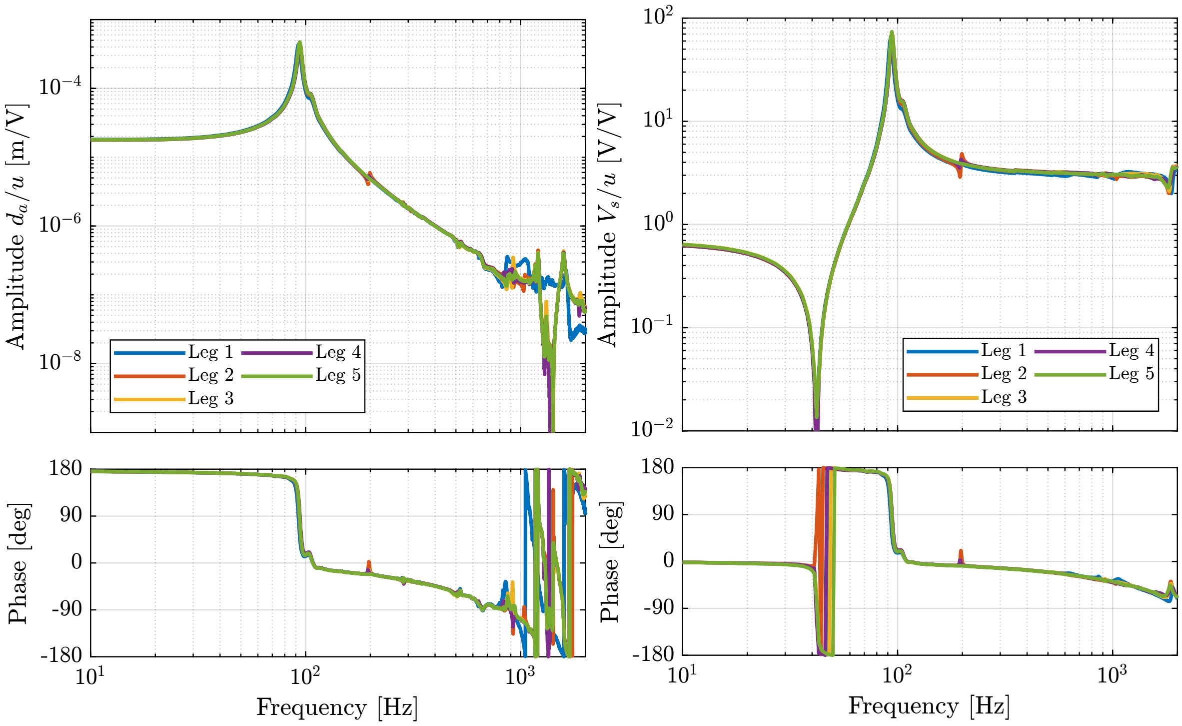

(a) u to d_a

(b) u to V_s

Figure 3.5: Comparison of the measured plants

The same comparison is made for the transfer function from u to d_e (encoder output) in Figure 3.6. This time, large dynamics differences are observed between the 5 struts. Even-though the same peaks are seen for all of the struts (95Hz, 200Hz, 300Hz, 400Hz), the amplitude of the peaks are not the same. Moreover, the location or even the presence of complex conjugate zeros is changing from one strut to the other.

It will be further investigated why such differences are observed (see Section 4.2).

Conclusion

Important

All the struts are giving very consistent behavior from the excitation voltage u to the force sensor generated voltage V_s and to the interferometer measured displacement d_a. However, the dynamics from u to the encoder measurement d_e is much more complex and variable from one strut to the other. The reason behind this variability will be studied in the next section thanks to the model of the strut.

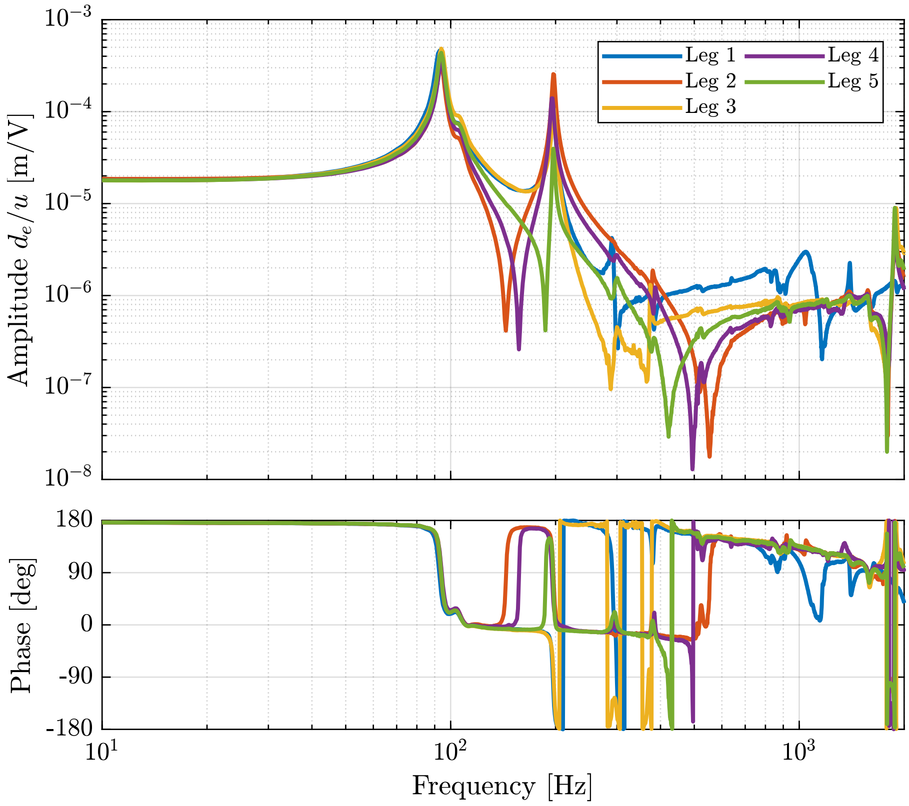

Figure 3.6: Estimated frequency response functions from u to the encoder d_e for all the mounted struts

4 Strut Model

However, now the full strut is put instead of only the APA (see Figure 4.1).

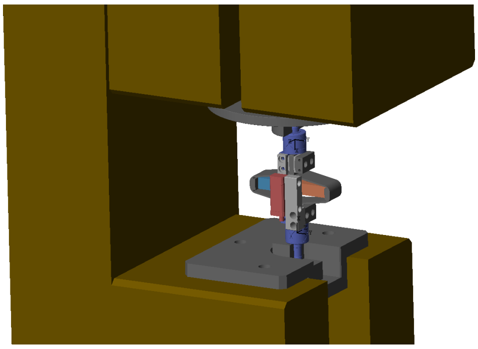

Figure 4.1: Screenshot of the Simscape model of the strut fixed to the bench

This Simscape model is used to:

- compare the measured FRF with the modelled FRF
- help the correct understanding/interpretation of the results
- tune the model of the struts (APA, flexible joints, encoder)

This study is structured as follow:

- Section 4.1: the measured FRF are compared with the Simscape model.
- Section 4.2: the flexible APA model is used, and the effect of a misalignment of the APA and flexible joints is studied. It is found that the misalignment has a large impact on the dynamics from u to d_e.
- Section 4.5: the effect of the flexible joint's stiffness on the dynamics is studied. It is found that the axial stiffness of the joints has a large impact on the location of the zeros on the transfer function from V_s to d_e.

4.1 Model dynamics

Two models of the APA300ML are used here for comparison:

- a simple two degrees of freedom model

- a model using a super element extracted from a finite element model

These two models of the APA300ML were tuned to best match measured frequency response functions of the APA alone. The flexible joints are here modelled with the 4DoF model (axial stiffness, two bending stiffnesses and one torsion stiffness).

These two models are compared with the measured frequency responses in Figure 4.2.

The model dynamics from DAC voltage u to the axial motion of the strut d_a (Figure 4.2a) and from DAC voltage u to the force sensor voltage V_s (Figure 4.2c) are well matching the experimental identification.

However, the transfer function from u to encoder displacement d_e are not well matching for both models. For the 2DoF model, this is normal as the resonances affecting the dynamics are not modelled at all (the APA300ML is modelled as infinitely rigid in all directions except the translation along it's actuation axis). For the flexible model, it will be shown in the next section that by adding some misalignment betwen the flexible joints and the APA300ML, this model can better represent the observed dynamics.

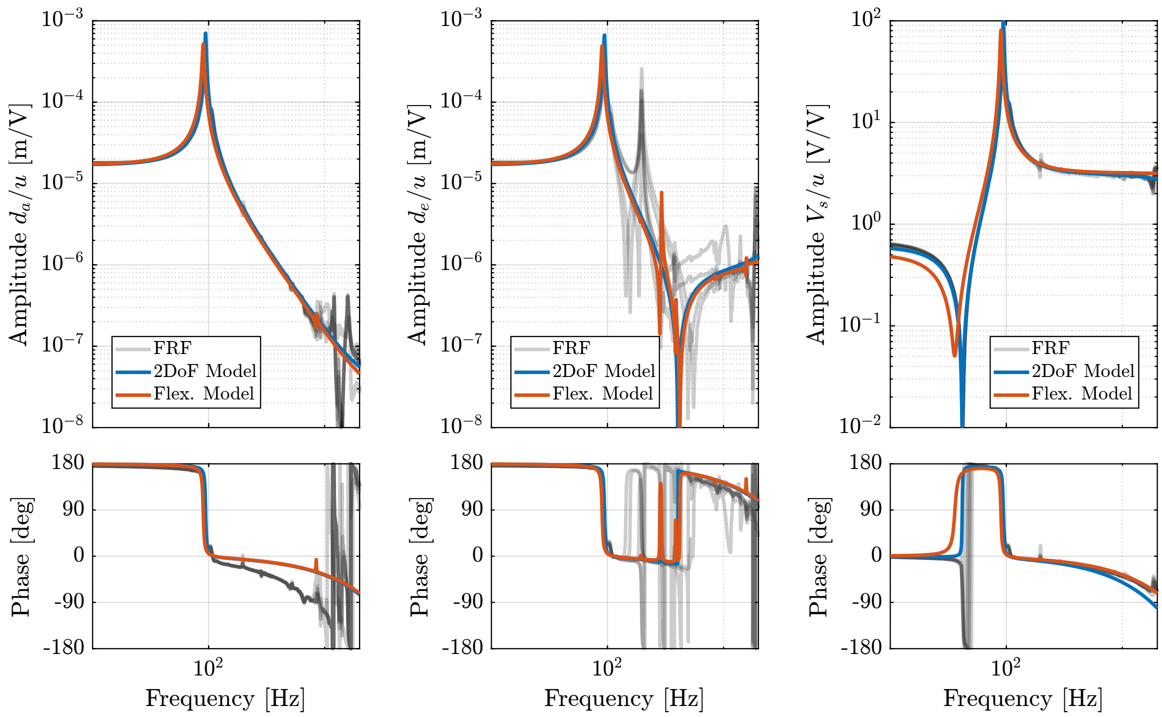

(a) u to d_a **(b)** u to d_e **(c)** u to V_s

Figure 4.2: Comparison of the measured dynamics and of the Simscape dynamics using the "flexible" APA300ML model (Super-Element extracted from a Finite Element Model).

4.2 Effect of strut misalignment

As was shown in Figure 3.6, the identified dynamics from DAC voltage u to encoder measured displacement d_e are very different from one strut to the other.

In this section, it is investigated whether poor alignment of the strut (flexible joints with respect to the APA) can explain such dynamics. For instance, consider Figure 4.3 where there is a misalignment in the y direction between the two flexible joints (well aligned thanks to the mounting procedure in Section 1) and the APA300ML. In such case, the "x-bending" mode at 200Hz (see Figure 2.2a) can be expected to be more excited, and thus the dynamics from the actuator to the encoder should be affected at frequencies around 200Hz.

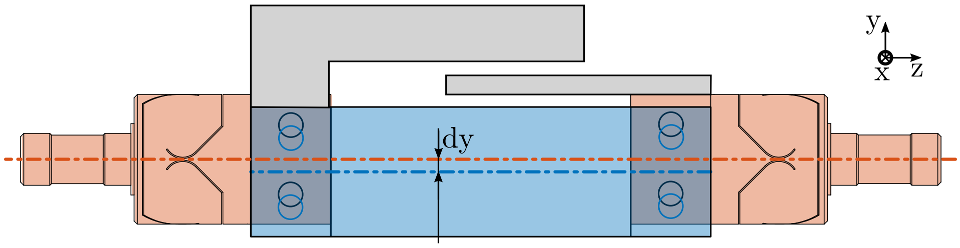

Figure 4.3: Mis-alignement between the joints and the APA

To verify this assumption, the dynamics from output DAC voltage u to the measured displacement by the encoder d_e is computed using the Simscape model with flexible APA for several misalignment in the y direction. Obtained dynamics are shown in Figure 4.4a. The alignment of the APA with the flexible joints as a **huge** influence on the dynamics from actuator voltage to measured displacement by the encoder. The misalignment in the y direction mostly influences:

- the presence of the flexible mode at 200Hz (see mode shape in Figure 2.1a)
- the location of the complex conjugate zero between the first two resonances:
  - if $d_y < 0$: there is no zero between the two resonances and possibly not even between the second and third ones
  - if $d_y > 0$: there is a complex conjugate zero between the first two resonances
- the location of the high frequency complex conjugate zeros at 500Hz (secondary effect, as the axial stiffness of the joint also has large effect on the position of this zero)

The same can be done for a misalignment in the x direction. The obtained dynamics are shown in Figure 4.4b where it is shown that misalignment in the x direction mostly influences the presence of the flexible mode at 300Hz (see mode shape in Figure 2.1b).

Comparing the experimental frequency response functions for all the APA in Figure 3.6 with the model dynamics for several y misalignments in Figure 4.4a indicates a clear similarity. This similarity suggests that the identified differences in dynamics are caused by the misalignment.

4.3 Measured strut misalignment

During the first mounting of the struts presented in Section 1, the positioning pins used to position the APA with respect to the flexible joints in the y directions were not used (not received at the time). Therefore, large y misalignments may be expected.

In order to estimate the misalignments between the two flexible joints and the APA:

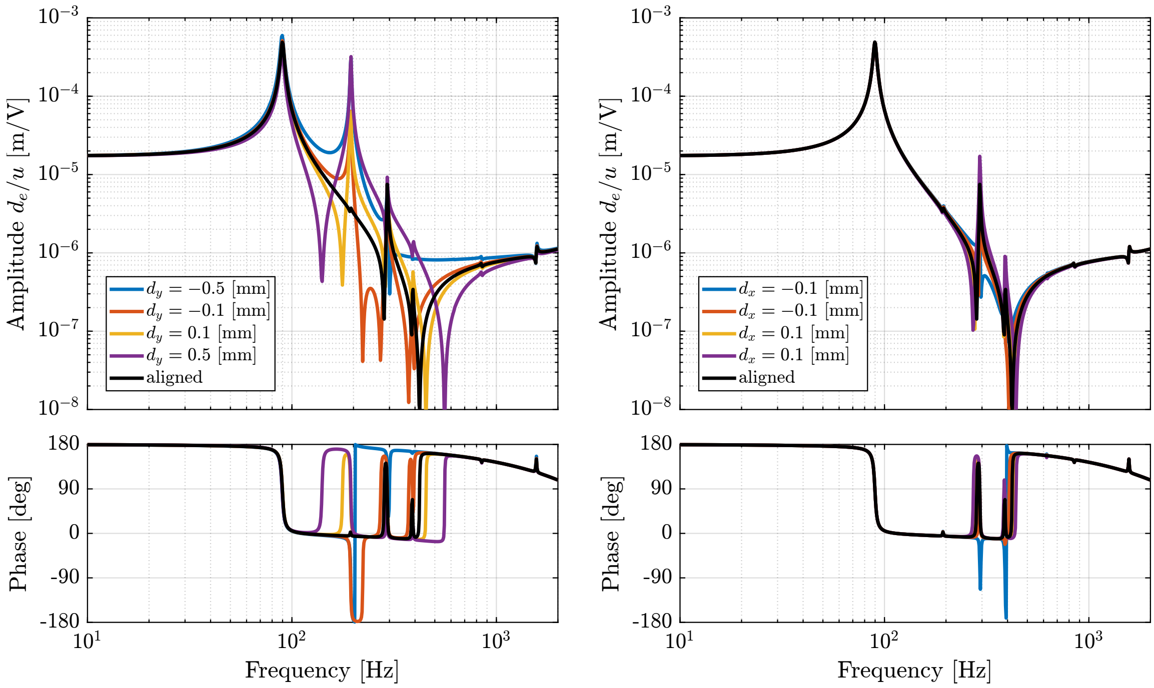

(a) Misalignment along y

(b) Misalignment along x

Figure 4.4: Effect of a misalignment between the flexible joints and the APA300ML in the y direction (a) and in the x direction (b)

- the struts are fixed horizontally to the mounting bench as shown in Figure 1.4c but without the encoder
- using a length gauge[1], the height difference from the flexible joints surface and the APA shell surface is measured both for the top and bottom joints and on both sides
- as the thickness of the flexible joint is $21\,mm$ and the thickness of the APA shell is $20\,mm$, $0.5\,mm$ of height different should be measured is the two are perfectly aligned

Large variations in the y misalignment are found from one strut to the other (results are summarized in Table 4.1).

To check the validity of the measurement, it can be verified that sum of the measured thickness difference on each side is $1\,mm$ (equal to the thickness difference between the flexible joint and the APA). This thickness differences for all the struts were found to be between $0.94\,mm$ and $1.00\,mm$ which indicate low errors as compared to the misalignments found in Table 4.1.

Table 4.1: Measured y misalignment at the top and bottom of the APA. Measurements are in mm

Strut	Bot	Top
1	0.1	0.33
2	-0.19	0.14
3	0.41	0.32
4	-0.01	0.54
5	0.15	0.02

By using the measured y misalignment in the Simscape model with the flexible APA model, the measured dynamics from u to d_e can be approached as shown in Figure 4.5. Even better match in the dynamics can be obtained by fine tuning both the x and y misalignments (yellow curves in Figure 4.5).

This confirms that the misalignment between the APA and the strut axis (determined by the two flexible joints) is critical and is inducing large variations in the dynamics from DAC voltage u to encoder measured displacement d_e. If encoders are to be used when fixed on the struts, it is therefore very important to properly align the APA and the flexible joints when mounting the struts.

In the next section, the struts are re-assembled with a "positioning pin" to better align the APA with the flexible joints. With a better alignment, the amplitude of the spurious resonances are expected to decrease as was shown in Figure 4.4a.

4.4 Proper struts alignment

After the positioning pins had been received, the struts were mounted again with the positioning pins. This should make the APA better aligned with the two flexible joints.

This alignment is then estimated using a length gauge as in the previous sections. Measured y alignments are summarized in Table 4.2 and are found to be bellow $55\mu m$ for all the struts which is much better than better (see Table 4.1).

[1] Heidenhain MT25, specified accuracy of $\pm 0.5\,\mu m$

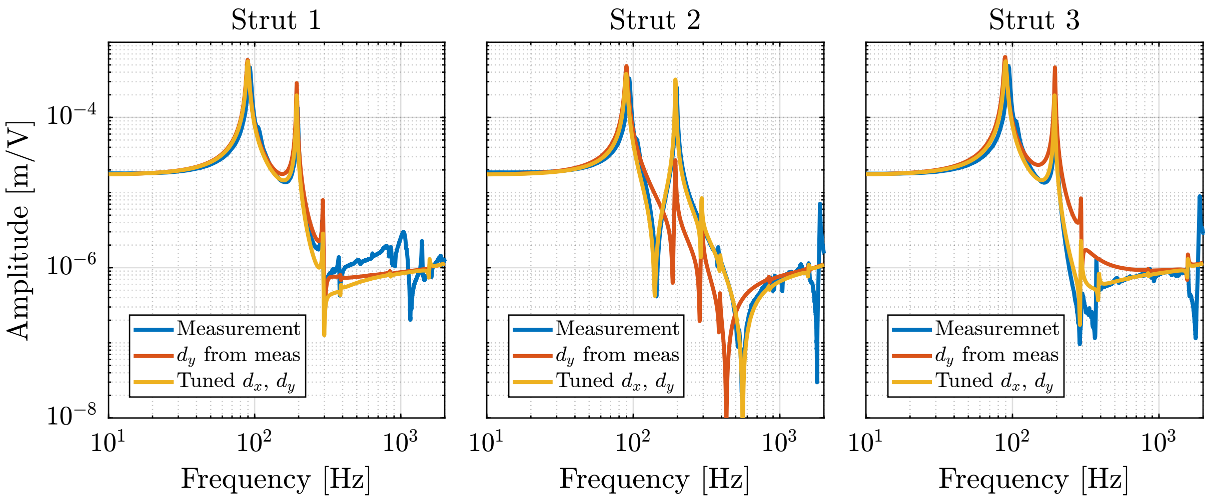

Figure 4.5: Comparison of the frequency response functions from DAC voltage u to measured displacement d_e by the encoders for three struts. In blue the measured dynamics, in red the dynamics extracted from the model with the y misalignment estimated from measurements, in yellow the dynamics extracted from the model when both the x and y misalignments are tuned

Table 4.2: Measured y misalignment at the top and bottom of the APA after realigning the struts using a positioning pin. Measurements are in mm.

Strut	**Bot**	**Top**
1	-0.02	0.01
2	0.055	0.0
3	0.01	-0.02
4	0.03	-0.03
5	0.0	0.0
6	-0.005	0.055

The dynamics of the re-aligned struts are then measured using the same test bench (Figure 3.1). The comparison of the initial strut dynamics and the dynamics of the re-aligned struts (i.e. with the positioning pin) is made in Figure ??.

Even though the struts are now much better aligned, not much improvement can be observed. The dynamics of the six aligned struts are quite different from one another.

Having the encoders fixed to the struts may prove to be difficult to use. Therefore, the encoders may be fixed to the nano-hexapod plates instead.

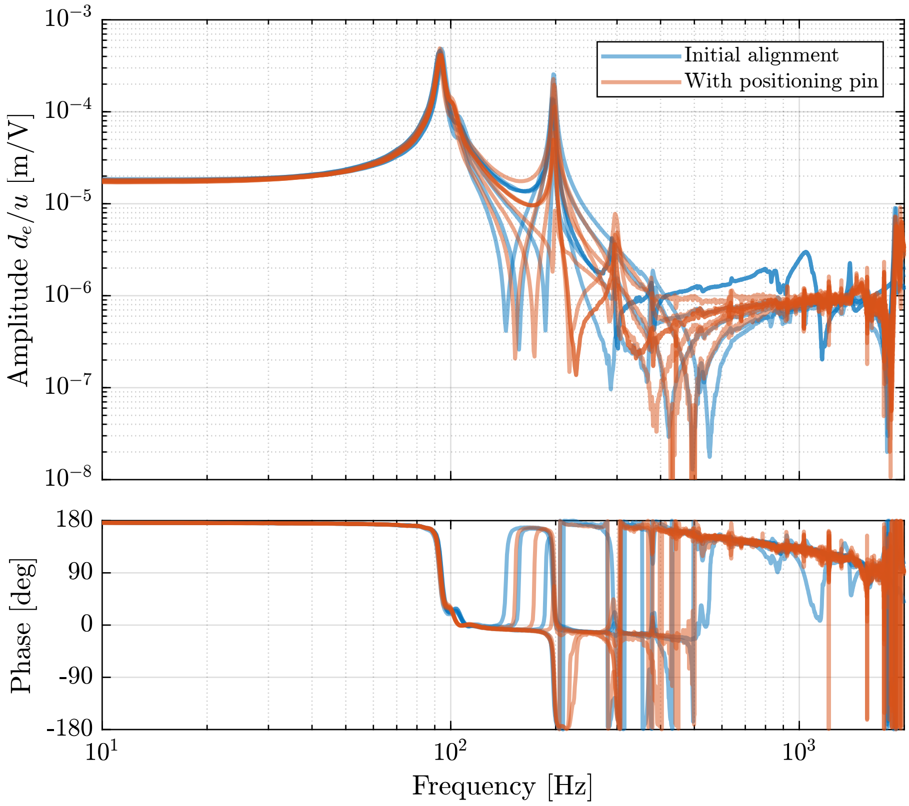

4.5 Effect of the flexible joint

As the struts are composed of one APA and two flexible joints, it is expected that the flexible joint characteristics will change the dynamic behavior of the struts.

Using the Simscape model, the effect of the flexible joint's characteristics on the dynamics as measured on the test bench are studied. The studied dynamics is between u and the encoder displacement d_e.

Let's initialize an APA which is a little bit misaligned.

The bending stiffness of the joints has little impact on the transfer function from u to d_e.

The axial stiffness of the flexible joint has a large impact on the frequency of the complex conjugate zero. Using the measured FRF on the test-bench, if is therefore possible to estimate the axial stiffness

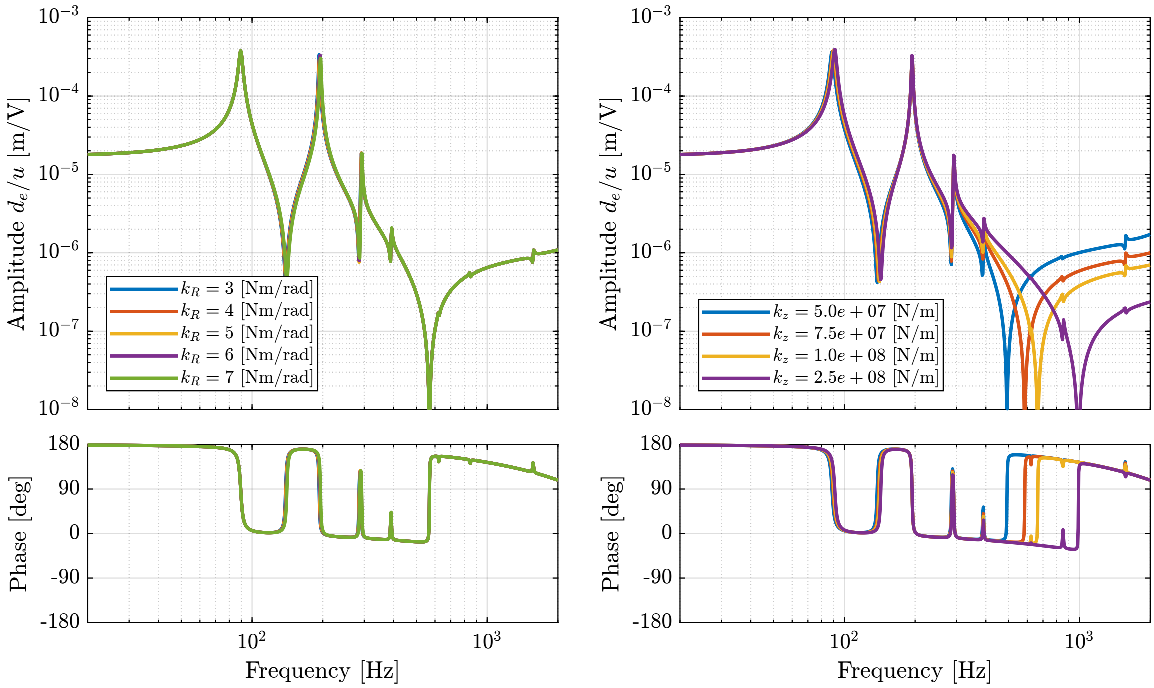

(a) Effect of bending stiffness

(b) Effect of axial stiffness

Figure 4.6: Effect of the flexible joints' bending (a) and axial (b) stiffnesses on the strut dynamics from u to d_e

of the flexible joints from the location of the zero.

This method gives nice match between the measured FRF and the one extracted from the simscape model, however it could give not so accurate values of the joint's axial stiffness as other factors are also influencing the location of the zero.

Using this method, an axial stiffness of $70 N/\mu m$ is found to give good results (and is reasonable based on the finite element models).

Conclusion

5 Conclusion